

High-throughput elucidation of thrombus formation reveals sources of platelet function variability

Johanna P. van Geffen,¹ Sanne L.N. Brouns,¹ Joana Batista,^{2,3} Harriet McKinney,^{2,3} Carly Kempster,^{2,3} Magdolna Nagy,¹ Suthesh Sivapalaratnam,^{2,4} Constance C.F.M.J. Baaten,¹ Nikki Bourry,¹ Mattia Frontini,^{2,3,5} Kerstin Jurk,⁶ Manuela Krause,⁷ Daniele Pillitteri,⁷ Frauke Swieringa,¹ Remco Verdood,¹ Rachel Cavill,⁸ Marijke J. E. Kuijpers,¹ Willem H. Ouwehand,^{2,3,5,9,10} Kate Downes^{2,3,9*} and Johan W.M. Heemskerk^{1*}

¹Department of Biochemistry, Cardiovascular Research Institute Maastricht (CARIM), Maastricht University, the Netherlands; ²Department of Haematology, University of Cambridge, Cambridge Biomedical Campus, UK; ³National Health Service Blood and Transplant (NHSBT), Cambridge Biomedical Campus, UK; ⁴The Royal London Haemophilia Centre, London, UK; ⁵BHF Centre of Excellence, Division of Cardiovascular Medicine, Cambridge University Hospitals, Cambridge Biomedical Campus, UK; ⁶Center for Thrombosis and Hemostasis (CTH), University Medical Center of the Johannes Gutenberg University Mainz, Germany; ⁷DKD Helios Klinik Wiesbaden, Germany; ⁸Department of Data Science & Knowledge Engineering, Faculty of Humanities and Sciences, Maastricht University, the Netherlands; ⁹NIHR BioResource, University of Cambridge, Cambridge Biomedical Campus, UK and ¹⁰Department of Human Genetics, The Wellcome Sanger Institute, Hinxton, Cambridge, UK

*KD and JWMH contributed equally to this work.

©2019 Ferrata Storti Foundation. This is an open-access paper. doi:10.3324/haematol.2018.198853

Received: May 31, 2018.

Accepted: December 5, 2018.

Pre-published: December 13, 2018.

Correspondence: JOHAN W. M. HEEMSKERK - jwm.heemskerk@maastrichtuniversity.nl

KATE DOWNES - kd286@cam.ac.uk

SUPPLEMENTARY INFORMATION

High-throughput elucidation of thrombus formation reveals sources of platelet function variability

Johanna P. van Geffen¹, Sanne L.N. Brouns¹, Joana Batista^{2,3}, Harriet McKinney^{2,3}, Carly Kempster^{2,3}, Magdolna Nagy¹, Suthesh Sivapalaratnam^{2,4}, Constance C. F.M.J. Baaten¹, Nikki Boury¹, Mattia Frontini^{2,3,5}, Kerstin Jurk⁶, Manuela Krause⁷, Daniele Pillitteri⁷, Frauke Swieringa¹, Remco Verdoold¹, Rachel Cavill⁸, Marijke J. E. Kuijpers¹, Willem H. Ouwehand^{3,4,9,10}, Kate Downes^{2,3*}, Johan W.M. Heemskerk^{1*}

*Equal contribution

Correspondence: Johan W. M. Heemskerk, PhD, Dept. of Biochemistry, CARIM, Maastricht University, P.O. Box 616, 6200 MD Maastricht, the Netherlands. Tel. +31-43-3881671, e-mail: jwm.heemskerk@maastrichtuniversity.nl and Kate Downes, Department of Haematology, University of Cambridge, NHS Blood and Transplant, Cambridge, CB2 0PT, UK, e-mail kd286@cam.ac.uk

Materials and Methods

Blood donors and blood collection

Studies were approved by the Maastricht University Medical Centre Ethics Committee and the Cambridge East Research Ethics Committee (Genetic analysis of platelets in healthy individuals, REC ref 10/H0304/65). Healthy subjects (laboratory population) in cohort 1 ($n = 10$) donated 3 blood samples at 2-4 weeks intervals. Genotyped healthy donors (cohort 2, $n = 94$) were analysed in a period of 2 weeks. These donors were registered in the National Institute for Health Research (NIHR) BioResource population; subjects were selected based on blood type O (to prevent blood type-linked differences in von Willebrand factor levels). All donors indicated not having taken antiplatelet medication during at least 2 weeks, and gave full informed consent according to the Helsinki declaration. Smoking or birth control was not recorded. Venous blood was collected in 5 mL vacutainers containing 3.2% trisodium citrate

or EDTA (for blood cell count assessment). The first 3 mL of blood were discarded to avoid platelet activation. After collection, blood samples were processed within 30 minutes after venepuncture for flow cytometry, immuno-phenotyping and measurement of haematological parameters. Independent samples were used within 2 hours for high-throughput assaying of thrombus formation. Patient blood samples, along with day control samples from healthy subjects, were obtained from outpatient clinics of University Medical Centre of the Johannes Gutenberg University Mainz and the Helios Klinik Wiesbaden, Germany, following full informed consent.

Haematological parameters

Blood samples collected on EDTA (cohort 2, patients and day controls) were used for measurements of haematological parameters using a Sysmex XN-1000 analyser (Sysmex Corporation, Kobe, Japan).

Genotyping of subjects of cohort 2

Genotyping of healthy blood donors (cohort 2) was performed as described.¹ Briefly, arrays of Illumina and Affymetrix genome-wide SNV genotyping were used to establish an encompassing set of variants using the 1,000 Genomes Project database, as a reference.² Regression analysis was performed to identify platelet traits that were associated with assumed relevant SNVs.¹

Preparation of microspot surfaces for microfluidics

Microspots surfaces were prepared according to standard operation proceedings such as indicated elsewhere,³ and detailed below. Glass coverslips were cleaned, after which platelet-adhesive proteins were applied as three adjacent 1.2 μm microspots (3 mm centre-to-centre distance) using a high-precision mould. Coating concentrations of all applied proteins were optimised, as described before.⁴ Using two coverslips, a total of six different microspots *M1-6* could be used, for functional detection of the most relevant platelet receptors (in brackets), as previously assessed.⁴ These were: *M1*, collagen type I (GPIIb, GPVI, $\alpha_2\beta_1$), applied at 100 $\mu\text{g}/\text{mL}$ (Horm, Takeda, Hoofddorp, The Netherlands); *M2*, collagen type III (GPIIb, GPVI, $\alpha_2\beta_1$), applied at 100 $\mu\text{g}/\text{mL}$ (Octapharma, Berlin, Germany); *M3*, VWF (GPIIb) + laminin ($\alpha_6\beta_1$), applied at 50 and 100 $\mu\text{g}/\text{mL}$, respectively (laminin: Sigma-Aldrich, 511/521, Zwijndrecht, The Netherlands); *M4*, VWF-BP (GPIIb) + GFOGER-(GPO)_n (GPVI, $\alpha_2\beta_1$), applied at 100 $\mu\text{g}/\text{mL}$ and 250 $\mu\text{g}/\text{mL}$ (both from Dept. of Biochemistry, University of Cambridge, UK);⁴ *M5*, VWF-BP (GPIIb) + rhodocytin (CLEC-2), applied at 100 and 250 $\mu\text{g}/\text{mL}$ (rhodocytin: a generous gift of Dr. K. Clemetson, Bern University);⁵ *M6*, VWF-BP (GPIIb) + human fibrinogen ($\alpha_{11b}\beta_3$), applied at 100 and 250 $\mu\text{g}/\text{mL}$ (fibrinogen: Sigma-

Aldrich F-4129-16). No cross-over effects were observed between the consecutive microspots.⁴ After incubation in a humid chamber for 1 hour at room temperature and blocking for 30 minutes with 1% bovine serum albumin blocking buffer, the coverslips were rinsed with saline and used for microfluidic studies.

Whole blood perfusion over microspots

Microfluidics assays were performed basically as before,⁴ using established protocols.³ Standard operation proceedings included the following modifications. Microspot-coated coverslips were mounted into a parallel-plate perfusion chamber (Maastricht flow chamber, depth 50 μm , width 3 μm , length 30 mm).⁶ Citrated blood samples (350 μL) were recalcified with 40 μM D-phenylalanyl-L-prolyl-L-arginine chloromethylketone, 3.75 mM MgCl_2 and 7.5 mM CaCl_2 , and then perfused for 3.5 minutes at a wall shear rate of 1000 s^{-1} (or 1600 s^{-1} , where indicated). Individual flow runs were performed with microspots *M6-M2-M1*, *M3-M2-M1* or *M6-M5-M4* (in the direction of blood flow). During a 1.5 minute perfusion with staining solution, two representative brightfield images per microspot were captured. Staining solution was composed of rinse buffer - 10 mM Hepes pH 7.45, 136 mM NaCl, 2.7 mM KCl, 2 mM MgCl_2 , 2 mM CaCl_2 , 1 mg/mL glucose, 1 mg/mL BSA, 5 U/mL fragmin (Pfizer) and 1 U/mL heparin (Sigma-Aldrich), containing FITC-labelled anti-fibrinogen mAb (1:100, Dako, F0111, Santa Clara, CA, USA), Alexa Fluor (AF)568 annexin A5 (1:200, Molecular Probes), and AF647 anti-CD62P mAb (1:80, Biologend, London, UK). After 2 minutes of stasis, unbound label was removed by post-perfusion with label-free rinse buffer. Subsequently, 3 representative fluorescence images per label and microspot were immediately captured under flow from in-focus fields of view. Low-wavelength pre-illumination was omitted in order to prevent fluorescence bleaching

Brightfield and 3-colour fluorescence images were taken with two equivalent EVOS-FL microscopes (Life Technologies), equipped with GFP, RFP and Cy5 LEDs and dichroic cubes, an Olympus UPLSAPO 60x oil-immersion objective, and a sensitive CCD camera (1360 \times 1024 pixels). Microscopes were used at standard settings of illumination and camera chip sensitivity.

Duplicate flow runs were performed, whenever possible. Test variability was 5-8%, depending on surface and parameter. To eliminate artefacts, flow runs were discarded and repeated if: (i) one or more of the coated microspots was physically damaged (no platelet adhesion), (ii) after recalcification blood clots were observed, (iii) air bubbles appeared in the flow channels, (iv) staining artefacts precluded proper quantification.

Quantitative image analysis and delineation of outcome microfluidic parameters

Prior to analysis, semi-automated scripts, using a manual threshold setting, were written for

standardised image analysis in the open-access program Fiji (based on ImageJ). The scripts in ijm format are available upon request. For brightfield images and for each fluorescent label, separate scripts were designed with: (i) optimised fast Fourier transformation to reduce background noise; (ii) morphological vertical and horizontal dilate and erode steps to remove noise pixels and enhance the relevant structures; (iii) automated threshold settings to generate binary mask images; (iv) overlay images to verify by eye the binary images; and (v) back loops to re-set thresholds if the analysis was incorrect. Images were evaluated by observers, blinded to the condition (genotypes, other subject and platelet characteristics).

Brightfield images provided five outcome parameters: *P1*, platelet surface area coverage (%SAC), obtained from threshold, binary images, representing identified regions of all adhered platelet and thrombus structures; *P2*, platelet aggregate %SAC, representing identified regions of multi-layered platelets; *P3*, thrombus morphological score (scale 0-5); *P4*, thrombus multilayer score (scale 0-3); *P5*, thrombus contraction score (scale 0-3). Scoring (half units) of the auto-enhanced brightfield images was based on a predefined gallery of typical images across microspots. Threshold, binary fluorescence images, indicative of platelet activation stages, gave %SAC per label: *P6*, PS exposure (AF568-annexin A5); *P7*, P-selectin expression (AF647 anti-CD62P mAb); *P8*, integrin $\alpha_{IIb}\beta_3$ activation (FITC anti-fibrinogen mAb). Adequacy of the transfer of image analysis data into Excel spreadsheets for data processing was checked by an independent observer.

Platelet immuno-phenotyping

Platelet immuno-phenotyping was performed using antibodies at recommend concentrations for the markers: CD29 (integrin β_1 : 555443, Becton & Dickinson), CD36 (GPIV: IM0766U, Beckman Coulter), CD41a (integrin $\alpha_{IIb}\beta_3$ complex: 303706, Biolegend), CD41b (integrin α_{IIb} : 555469, Becton & Dickinson), CD42a (GPIX: 558819, Becton & Dickinson), CD42b (GPIIb: 551061, Becton & Dickinson), CD49b (integrin α_2 : 359308, Biolegend), CD61 (integrin β_3 : F0803, Dako), CD148 (11148942, eBiosciences). Data were analysed by Kaluza Flow Cytometry analysis software.⁷

For determination of GPVI expression, non-conjugated anti-GPVI antibody (clone HY101, 25 $\mu\text{g}/\text{mL}$) or the non-conjugated isotype control (IgG2a) were used, as described elsewhere.⁸ Platelets were incubated with a FITC-labelled F(ab')₂ secondary antibody at a final concentration of 50 $\mu\text{g}/\text{mL}$. Median fluorescence intensities of platelets incubated with anti-GPVI or control antibody were determined by flow cytometry and analysed using Kaluza software.

Platelet activation by flow cytometry

Flow cytometry experiments were performed as described.⁷ In brief, citrated blood samples

were incubated for 5 minutes with aspirin (100 μ M, Sigma-Aldrich), hirudin (10 U/mL, Sigma-Aldrich) and apyrase (4 U/mL, Sigma-Aldrich), as appropriate. After 1:10 dilution in HEPES-buffered saline (140 mM NaCl, 5 mM KCl, 1 mM MgSO₄, 10 mM HEPES, pH 7.4), samples were incubated for 20 minutes with either FITC-conjugated fibrinogen (F0111, Dako) or PE-conjugated anti-CD62P mAb (Thromb6, Bristol Institute for Transfusion Science, NHSBT Bristol, UK) in the presence of cross-linked collagen-related peptide (CRP-XL, 0.1 μ g/mL), ADP (0.5 μ M), or TRAP-6 (SFLLRN, 1.6 μ M). Platelet activation was stopped using formal saline (0.2% formaldehyde), prior to measurements using a FC500 flow cytometer (Beckman-Coulter) and analysis using Kaluza software.

Bioinformatics and statistics

Data are presented as means (with 95% confidence intervals). For heatmap analysis, mean values of defined outcome parameters from the microfluidics assay were linearly normalised to a range from 0-10 (majority of values were normally distributed, Suppl. Table 2). One-way unsupervised hierarchical clustering was performed using the R package version 3.2.5 (www.r-project.org). Euclidean distances were calculated and clustering was performed by complete linkages.

Data per cohort study were statistically analysed by probability analysis (Mann-Whitney U-test for numerical or continuous variables) using GraphPad Prism 6 software. Matrices of outcome parameters were compared by multiple correlation and regression analysis (cohort 2, $n = 94$). Specific pairs of parameters were compared by Spearman correlation analysis (2-tailed, $n = 94$). Given the high correlations between microspot parameters, Bonferroni corrections are too conservative for use.

To identify genotype associations, variables were quantile normalised and alleles tested for each variant using a likelihood ratio test under a univariate linear regression model. For the genetic variants, carriers and non-carriers of the less common allele were compared. Non-rotated principal component analysis was performed using the statistical package for social sciences (SPSS version 22). Therefore, raw data were employed for one- or two-principal component models to explain intra- and inter-individual variations. Using MatLab, prediction models were built for regression models with β -matrices; all models were checked by cross-validation predictions.

References

1. Petersen R, Lambourne JJ, Javierre BM, Grassi L, Kreuzhuber R, Ruklisa D, et al. Platelet function is modified by common sequence variation in megakaryocyte super enhancers. *Nat Commun.* 2017;8:16058.

2. The Genomes Project C. A global reference for human genetic variation. *Nature*. 2015;526:68-74.
3. De Witt S, Swieringa F, Cosemans JM, Heemskerk JW. Thrombus formation on microspotted arrays of thrombogenic surfaces. *Nat Protocol Exchange*. 2014;2014:3309#.
4. De Witt SM, Swieringa F, Cavill R, Lamers MM, van Kruchten R, Mastenbroek T, et al. Identification of platelet function defects by multi-parameter assessment of thrombus formation. *Nat Commun*. 2014;5:4257.
5. Hooley E, Papagrorgiou E, Navdaev A, Pandey AV, Clemetson JM, Clemetson KJ, et al. The crystal structure of the platelet activator aggretin reveals a novel $\alpha\beta_2$ dimeric structure. *Biochemistry*. 2008;47:7831-7.
6. Van Kruchten R, Cosemans JM, Heemskerk JW. Measurement of whole blood thrombus formation using parallel-plate flow chambers: a practical guide. *Platelets*. 2012;23:229-42.
7. Chen L, Kostadima M, Martens JH, Canu G, Garcia SP, Turro E, et al. Transcriptional diversity during lineage commitment of human blood progenitors. *Science (New York, NY)*. 2014;345:1251033.
8. Jones CI, Bray S, Garner SF, Stephens J, de Bono B, Angenent WG, et al. A functional genomics approach reveals novel quantitative trait loci associated with platelet signaling pathways. *Blood*. 2009;114:1405-16.

Suppl. Table 1. Demographics of healthy blood donors (cohort 2).

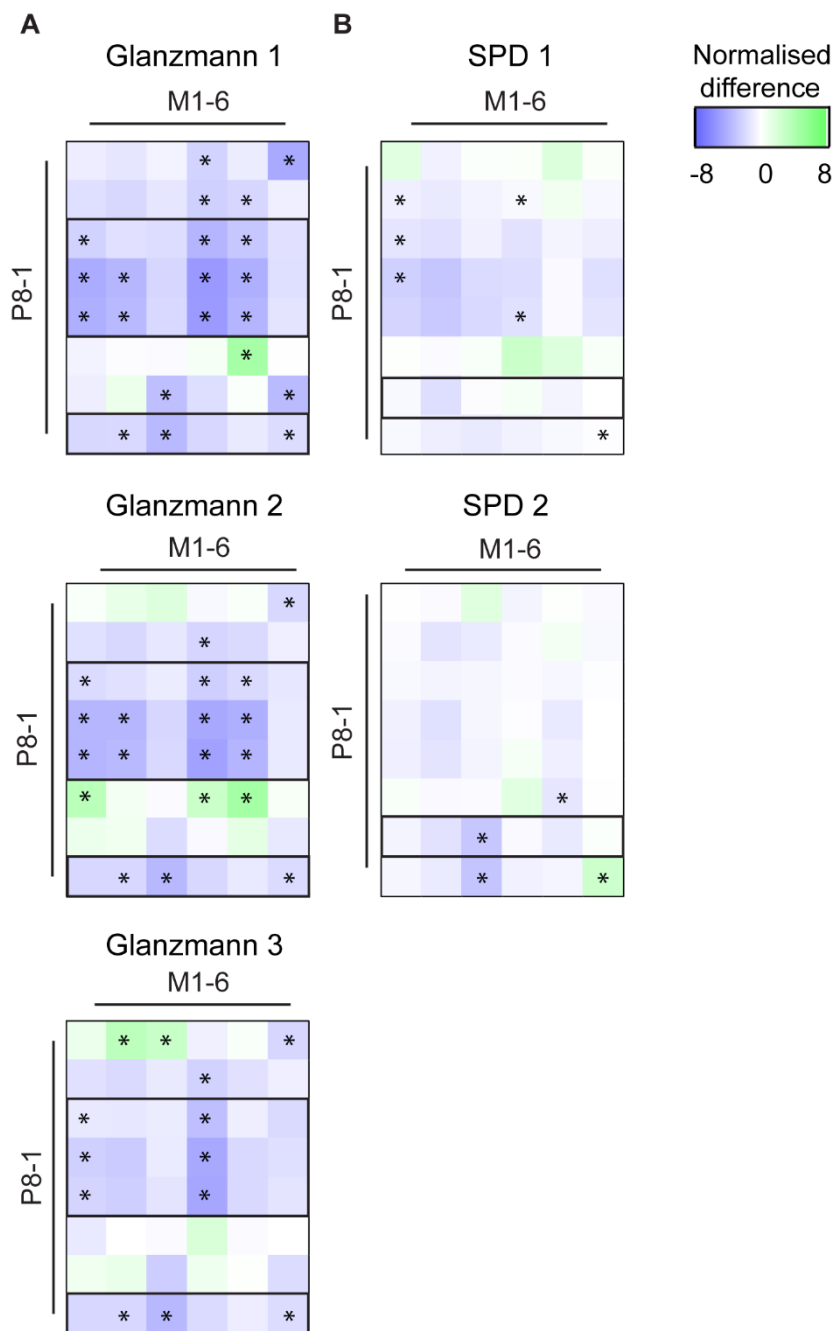
	Male	Female
Sex, n	36	58
Age, median (range)	64 (25 - 79)	64 (34 – 77)
Antithrombotic medication, n	0	0

Suppl. Table 2. Normal distribution of thrombus parameter values (cohort 2). P values of D'Agostino & Pearson omnibus normality test (colour cells with $p > 0.05$ indicate normal distribution).

	<i>P1</i>	<i>P2</i>	<i>P3</i>	<i>P4</i>	<i>P5</i>	<i>P6</i>	<i>P7</i>	<i>P8</i>
<i>M1</i>	0.2222	0.4009	0.2283	0.2571	0.4505	0.0016	0.9042	0.1879
<i>M2</i>	0.4115	0.0136	0.0322	0.2316	0.155	0.0001	0.991	0.0487
<i>M3</i>	0.7058	0.0015	0.0666	0.0446	0.0049	0.0001	0.0648	0.3702
<i>M4</i>	0.1337	0.554	0.7052	0.2332	0.7554	0.005	0.3618	0.3358
<i>M5</i>	0.8161	0.2338	0.5757	0.2943	0.1534	0.0001	0.0842	0.0017
<i>M6</i>	0.3127	0.0001	0.0001	0.0425	0.001	0.0001	0.0001	0.0001

Suppl. Table 3. Inter- and intra-individual variation on indicated microspots (*M*) and parameters (*P*) in whole blood thrombus formation of three separate blood samples from 10 healthy subjects (cohort 1). Coefficients of variation are given, expressed as fractions (mean values). Ratio values represent inter-individual variation divided by intra-individual variation.

	<i>P1</i>	<i>P2</i>	<i>P3</i>	<i>P4</i>	<i>P5</i>	<i>P6</i>	<i>P7</i>	<i>P8</i>
<i>Inter-individual variation</i>								
<i>M1</i>	0.22	0.40	0.10	0.09	0.09	0.62	0.27	0.44
<i>M2</i>	0.16	0.29	0.09	0.14	0.16	0.63	0.22	0.32
<i>M6</i>	0.56	0.90	0.17	0.42	0.57	0.89	0.74	0.90
<i>Intra-individual variation</i>								
<i>M1</i>	0.11	0.29	0.08	0.09	0.12	0.29	0.17	0.22
<i>M2</i>	0.18	0.23	0.09	0.19	0.16	0.44	0.18	0.17
<i>M6</i>	0.18	0.59	0.09	0.41	0.47	0.42	0.13	0.32
<i>Ratio</i>								
<i>M1</i>	2.45	0.94	1.11	1.75	1.44	2.18	1.39	1.45
<i>M2</i>	1.07	2.02	1.26	1.97	2.72	3.24	1.37	3.90
<i>M6</i>	3.97	1.49	2.99	1.59	1.83	4.25	9.05	3.96



Suppl. Figure 1. Alterations in thrombus formation in Glanzmann's thrombasthenia (GT) and delta storage pool disease (SPD). Blood from patients with GT1-3 (A-C) or SPD1-2 (D-E), or from 3 day controls (C1-3) was flowed over microspots *M1-6*, and thrombus parameters *P1-8* were evaluated. Quantification and data normalization was as described for Figure 2. Subtraction heatmaps indicate scaled values, compared to those from C1-3. Colour bars indicate relative increases or decreases; *changes outside the range of mean \pm 2 SD. Note consistent changes of platelet aggregation-linked parameters (*P2-5*, *P8*) across surfaces for

GT1-3.

Suppl. Data file 1. Inter-individual CVs for the 94 samples and intra-individual CVs from a subset of 10 of these samples on indicated microspots (M) and parameters (P) in whole blood thrombus formation (cohort 2). Coefficients of variation are given, expressed as fractions (mean values). Ratio values represent inter-individual variation divided by intra-individual variation (**A**). Raw data of whole blood thrombus formation (**B**) and subject age, sex, haematological data, platelet glycoprotein expression levels and agonist-induced platelet activation markers by flow cytometry (**C**) of 94 healthy individuals. Raw data of whole blood thrombus formation of patients' blood samples and their day controls (**D**).

Suppl. Data File 2. Full statistical data on Pearson's $-\log p$ values (**A, C**) and correlation coefficients (**B, D**) on whole blood thrombus formation parameters and on subject age, sex, haematological data, platelet glycoprotein expression levels and agonist-induced platelet activation markers by flow cytometry, respectively. Raw data on PCA matrix measurements (**E**).